CERAMIC PROCESSING STUDIES IN $MgAl_2O_4$ SYSTEM

Paul J. Jorgensen

Stanford Research Institute

Prepared for:

Naval Air Systems Command

January 1974

Security Classification

AD 777706

DOCUMENT CONTROL DATA - R & D

Security classification of title, body of abstract and indexing annotation must be entered when the overall report is classified

1. ORIGINATING ACTIVITY (Corporate author)
Stanford Research Institute
333 Ravenswood Avenue
Menlo Park, California 94025

2a. REPORT SECURITY CLASSIFICATION

2b. GROUP

3. REPORT TITLE
CERAMIC PROCESSING STUDIES IN $MgAl_2O_4$ SYSTEM

4. DESCRIPTIVE NOTES (Type of report and inclusive dates)
Final Technical Report

5. AUTHOR(S) (First name, middle initial, last name)
Paul J. Jorgensen

6. REPORT DATE	7a. TOTAL NO. OF PAGES	7b. NO. OF REFS
January 1974	42	30

8a. CONTRACT OR GRANT NO	9a. ORIGINATOR'S REPORT NUMBER(S)
N00019-71-C-0246	PYU-1123
b. PROJECT NO	
c.	9b. OTHER REPORT NO(S) (Any other numbers that may be assigned this report)
d.	

10. DISTRIBUTION STATEMENT
Approved for public release; distribution unlimited.

11. SUPPLEMENTARY NOTES	12. SPONSORING MILITARY ACTIVITY
	Naval Air Systems Command Department of the Navy Washington, D.C. 20360

13. ABSTRACT

The final-stage sintering behavior or densification of $MgAl_2O_4$ has been studied as a function of stoichiometry in an attempt to inhibit grain growth by solute segregation to the grain boundaries and to allow spinel to sinter to theoretical density. It was found that the grain growth could be inhibited by deviations from stoichiometry, and that grain growth inhibition increased as the spinel composition approached the solid solubility limit in MgO-rich spinel. The relative grain boundary velocity calculated from the grain growth data obeys Cahn's impurity drag model for low-velocity grain growth with a low driving force, if we assume that the oxide concentration in excess of the stoichiometric composition acts as the solute.

Changes in stoichiometry do not provide sufficient grain growth inhibition to prevent the occurrence of discontinuous grain growth. However, spinel can be sintered to theoretical density by a second-phase mechanism in which the second phase is MgO. The presence of the second phase in the spinel causes light scattering and results in a translucent material.

DD FORM 1 NOV 68 1473 (PAGE 1)

S/N 0101-807-6801

Unclassified

Security Classification

14 KEY WORDS	LINK A		LINK B		LINK C	
	ROLE	WT	ROLE	WT	ROLE	WT
Sintering						
Ceramic Processing						
Grain Growth						
Spinel						
Armor						

PYU-1123

CERAMIC PROCESSING STUDIES IN $MgAl_2O_4$ SYSTEM

by

PAUL J. JORGENSEN
Stanford Research Institute
333 Ravenswood Avenue
Menlo Park, California 94025

Copy No. 222

CONTENTS

TABLES

ILLUSTRATIONS

I INTRODUCTION

Studies of the atomic mechanisms of sintering of oxides have been primarily concerned with initial stage sintering, i.e., neck growth between spheres or initial shrinkage of powder compacts. This situation has resulted because of the ease of applying physical models to initial stage sintering. Technological interest, however, is centered on the final stages of sintering or on the ultimate densification of a powder compact, in which a geometrically more complex situation exists.

The importance of grain boundaries to intermediate and final stage sintering has been well recognized since the experiments of Alexander and Balluffi.[1] Subsequent experimental and theoretical treatments of the role of grain boundaries include the studies of Burke,[2] Seigle.[3] Van Bueren and Hornstra,[4] and Coble and Burke.[5]

The sintering of oxides during final densification may be regarded as a diffusion process in which the vacancies diffuse from the pores to the grain boundaries. The vacancies are eliminated at the grain boundaries, resulting in shrinkage and densification. A compacted powder may sinter to theoretical density if the vacancy flux from the pores to the boundaries can be maintained at a high level.

A high vacancy flux can be maintained by controlling the grain boundary motion, so that the distance between pores and grain boundaries remains relatively small or by modifying the defect structure so that diffusion of the rate limiting species is increased. If the reduction in grain boundary mobility is sufficient to maintain a relatively high vacancy flux, and simultaneously prevent discontinuous grain growth, sintering will proceed until theoretical density has been achieved. Sintering to theoretical

density has been achieved in Al_2O_3 by adding MgO,[6] in Y_2O_3 by adding ThO_2,[7] and in ThO_2 by adding either CaO[8] or Y_2O_3.[9]

Several mechanisms have been postulated to explain the effects of solute additions on final stage sintering, and these include (1) modification of the defect structure,[10] (2) solute segregation to grain boundaries resulting in a decreased grain boundary mobility,[11] and (3) the formation of a second phase which impedes grain boundary motion.[8] The last mechanism is believed to occur in the ThO_2-CaO system. The amount of solute required to achieve theoretical density in Al_2O_3, Y_2O_3 and ThO_2 doped with Y_2O_3 is less than the equilibrium solid solubility limit and therefore a second phase mechanism cannot explain the final stage sintering in these systems. Jorgensen and Anderson[7] invoked a solute segregation mechanism to explain the sintering of Y_2O_3 doped with ThO_2, and Reijnen[10] ascribed the phenomenon to a modified defect structure. Reijnen assumed that yttrium ions diffuse faster than oxygen ions in Y_2O_3 and reasoned that the cation deficient defect structure resulting from doping Y_2O_3 with ThO_2 would cause a decrease in the sintering rate and decreased grain growth. Figure 1 is a plot of the oxygen and yttrium diffusion coefficients in Y_2O_3 as a function of reciprocal temperature. Since yttrium ions are the slower diffusion species, Reijnen's hypothesis is incorrect. Furthermore, ThO_2 can be sintered to theoretical density by adding Y_2O_3 solute, and a model involving a higher diffusion flux between the pores and grain boundaries because of the formation of favorable defect structures cannot explain the sintering to theoretical density in both systems since cation diffusion is slower than anion diffusion in both Y_2O_3 and ThO_2.

Segregation of the solute to grain boundaries with the solute producing a drag on the grain boundary motion is the best available model to explain the inhibition of grain growth and sintering to theoretical density in Al_2O_3 and Y_2O_3. The grain boundary velocity decreases in Y_2O_3 as the solute concentration increases (see Fig. 2) and this phenomenon

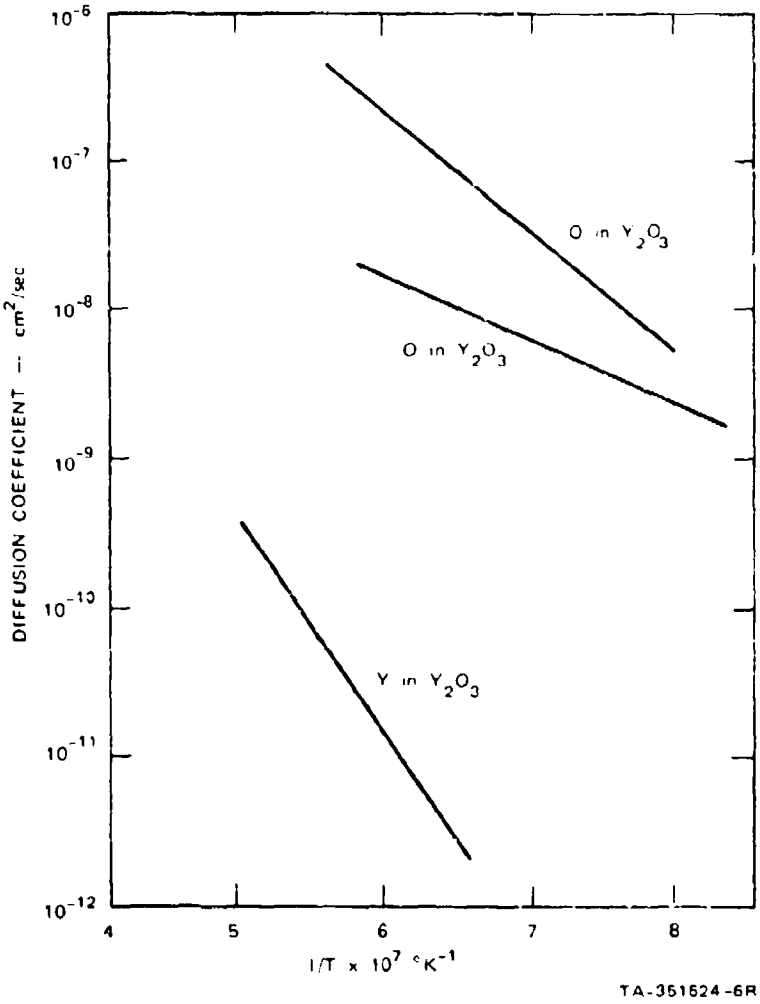

FIGURE 1 CATION AND ANION DIFFUSION COEFFICIENTS IN Y_2O_3 AS A FUNCTION OF RECIPROCAL TEMPERATURE

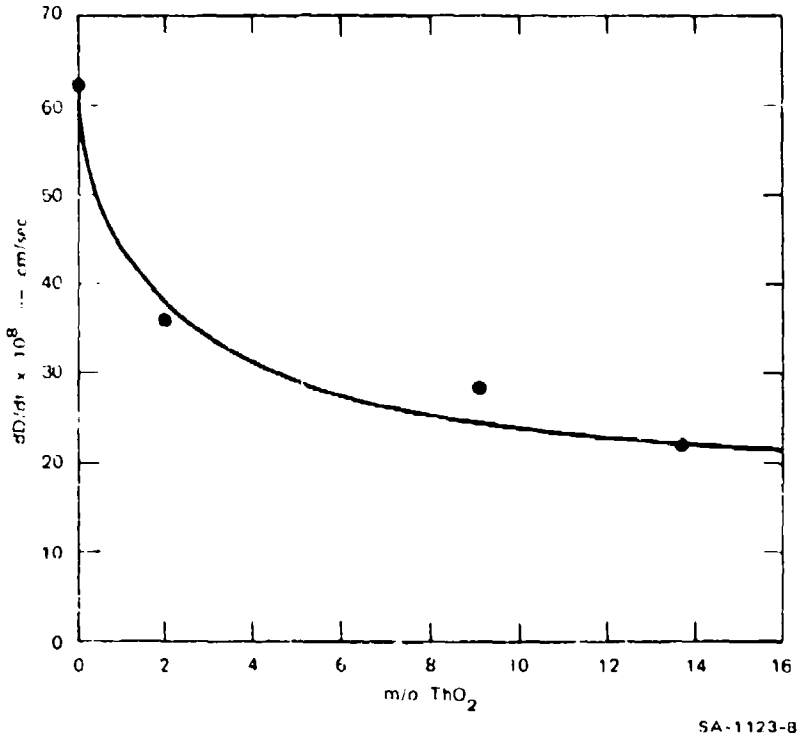

FIGURE 2 GRAIN BOUNDARY VELOCITY IN Y_2O_3 AT 2000°C AS A FUNCTION OF THORIA SOLUTE CONCENTRATION

has been treated theoretically by Cahn.[12] For low velocity grain boundary motion Cahn's theory gives the following relationship between grain boundary velocity, V, and solute concentration, C_o,

$$V = \frac{P}{\lambda + \alpha C_o} \qquad (1)$$

where P is the driving force for grain boundary motion, λ is an intrinsic drag coefficient, and α is a constant containing the reciprocal of the mobility multiplied by a summation of the adsorption energies of the solute on the grain boundary.

The solid line shown in Figure 2 is a curve calculated from Equation (1) force-fitted to the yttria sintering data, substituting the instantaneous grain growth rate dD/dt for the grain boundary velocity. Thus it appears that the ThO_2 solute in Y_2O_3 segregated to the grain boundaries and that the relative amount of segregation increases as the solid solubility limit is approached.

$MgAl_2O_4$, spinel, was selected as a system in which final stage sintering should be studied because of the wide range of solid solubility on both sides of the stoichiometric compound (see Fig. 3) and because the achievement of transparent polycrystalline spinel having a controlled microstructure could find application as an armor material.

Considerable work has been expended on studying the final stage sintering of $MgAl_2O_4$. Gatti et al.[13] produced a large-grained, transparent, spinel material by adding Li_2O and SiO_2 to $MgAl_2O_4$ using a firing schedule designed to remove the Li_2O and SiO_2 following complete densification. Bagley[14] has also produced a theoretically dense spinel material by adding MgO to $MgAl_2O_4$; however, this material is best described as translucent since the in-line transmission between wavelengths of 0.4 and 0.7 μm was approximately 9% for a 1-mm-thick sample.

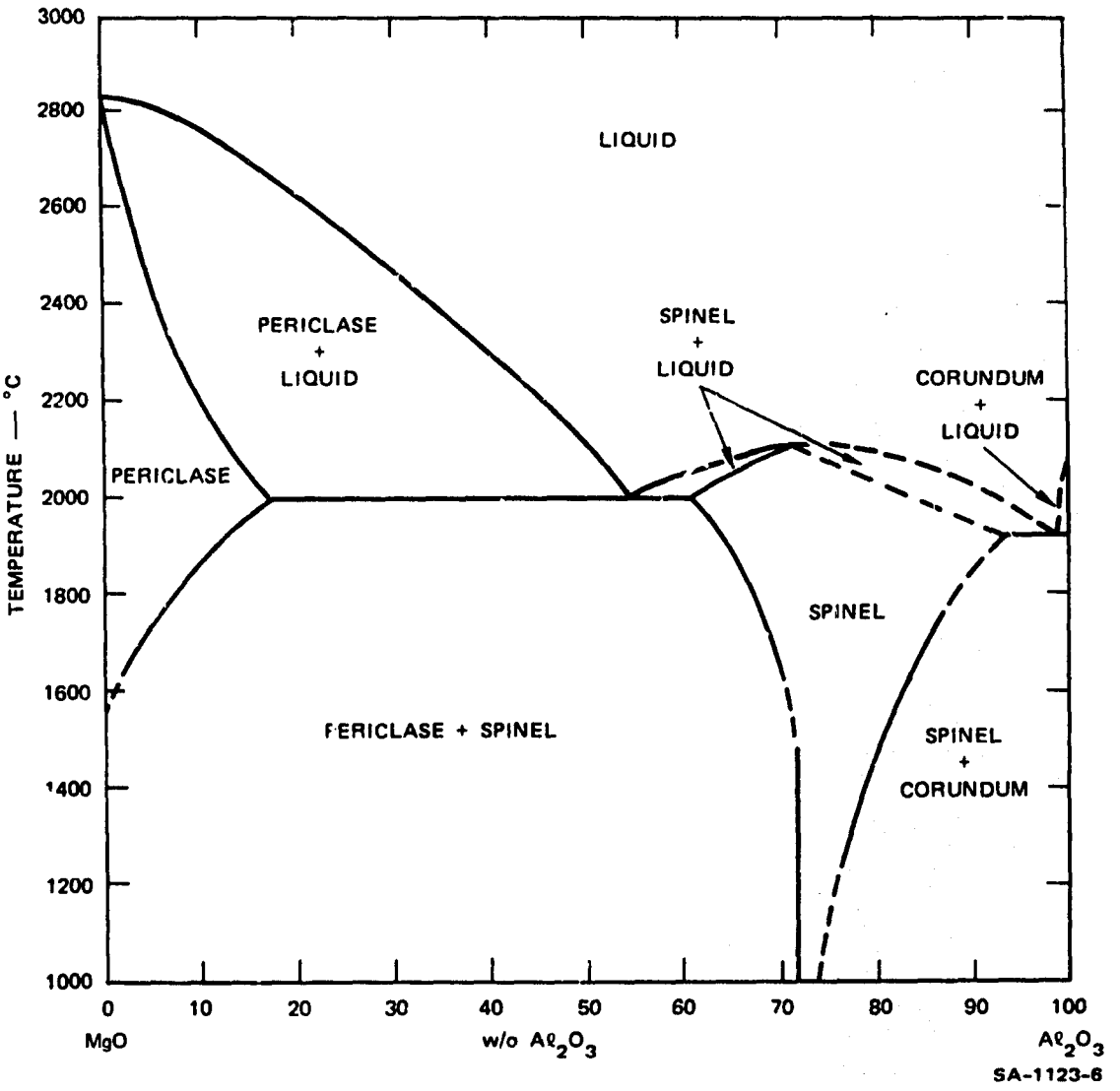

FIGURE 3 PHASE DIAGRAM FOR THE MgO $A\ell_2O_3$ SYSTEM (AFTER ROY ET AL[29] AND ALPER ET AL[30];

Bratton[15,16] has also studied the densification of $MgAl_2O_4$ including the initial stage sintering kinetics. He concluded that the sintering kinetics were controlled by a volume diffusion mechanism. Diffusion coefficients calculated from Bratton's initial sintering data are shown in Fig. 4. compared with some preliminary magnesium diffusion data,[17] and oxygen self-diffusion data.[18] Earlier oxygen diffusion data published by Ando and Oishi[19] were determined by analyzing the O^{18}/O^{16} ratio in the gas phase above solid spinel as functions of time and temperature without correcting for surface exchange. Correction of these data for surface exchange gave the oxygen diffusion coefficients shown in Fig. 4. An extrapolation of Bratton's calculated diffusion coefficients to higher temperatures shows good agreement with the oxygen self-diffusion data, indicating that the sintering kinetics are controlled by oxygen diffusion.

Aluminum ion diffusion has not been measured in $MgAl_2O_4$, but we expect the aluminum ions to diffuse faster than the oxygen ions and it is reasonable to expect oxygen to be the slowest diffusing species in the $MgAl_2O_4$ system, since oxygen ions are the slowest diffusing species in both MgO and Al_2O_3. Therefore, if volume diffusion processes control the final stage sintering or densification of spinel, we would expect the transport of oxygen to be rate limiting.

From the existing data on sintering of oxides such as Y_2O_3 and ThO_2, we can postulate that the segregation of a solute increases as the oxide composition approaches the solid solubility limit. The objectives of this study are to determine whether sintering of nonstoichiometric spinel with compositions approaching the solid solubility limit will exhibit a reduced grain boundary mobility and allow sintering to proceed to theoretical density.

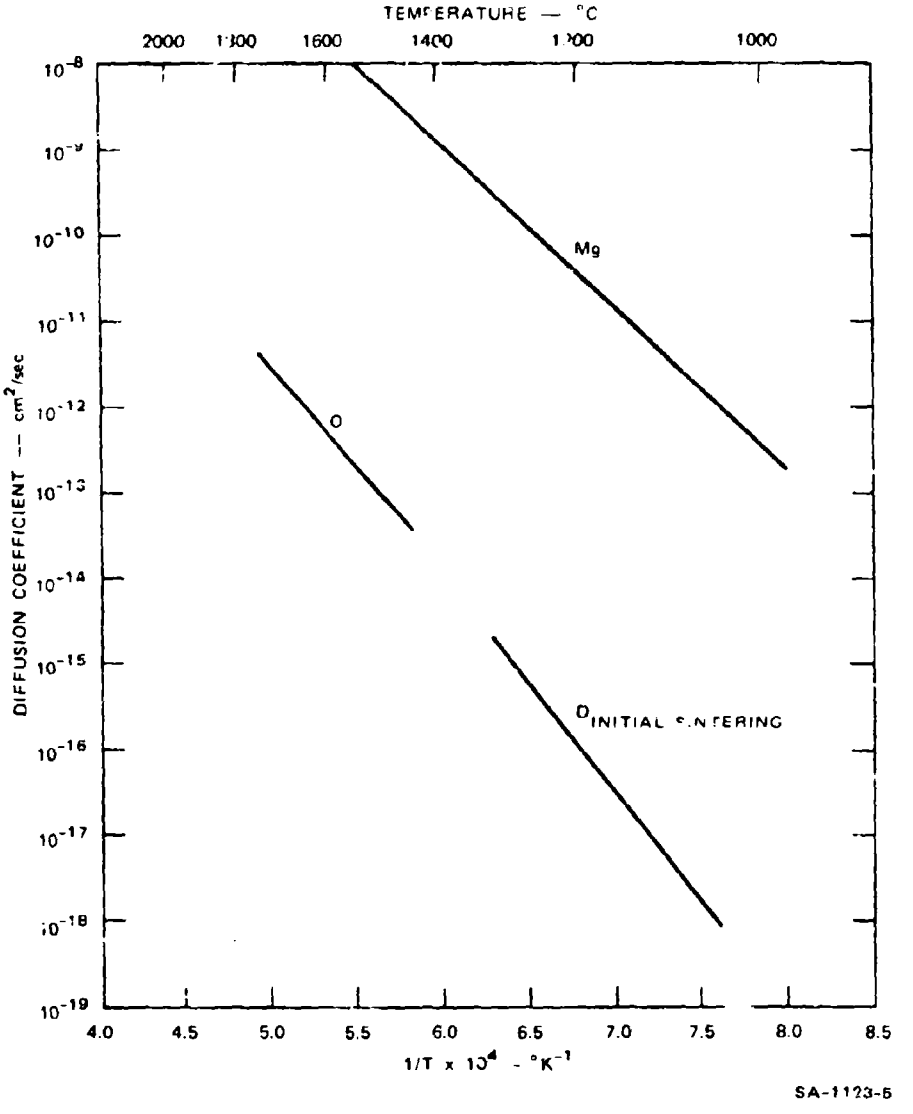

FIGURE 4 CATION AND ANION DIFFUSION COEFFICIENTS IN $MgAl_2O_4$ AS A FUNCTION OF RECIPROCAL TEMPERATURE COMPARED WITH DIFFUSION COEFFICIENTS CALCULATED FROM INITIAL STAGE SINTERING KINETICS

II SUMMARY AND CONCLUSIONS

The calcining of a mixture of hydrated ammonium aluminum sulfate and hydrated magnesium nitrate salts provides the most consistently reproducible method for producing submicron $MgAl_2O_4$ powder. These salts melt at approximately 95°C forming a liquid phase in which excellent mixing of the magnesium and aluminum ions occurs. Decomposition of the nitrate-sulfate mixture on heating to 1300°C for one hour results in a fine powder with an average particle size of approximately 0.3 μm.

Hydroxyl groups are incorporated in the spinel lattice during calcining and sintering. The concentration of the hydroxyl groups is inversely proportional to the MgO content of MgO-rich spinels, and it is suggested that a defect equilibrium forms in which two protons substitute for one magnesium ion.

Rapid pore coalescence occurs in spinel during sintering, and this pore coalescence allows the spinel grains to grow uninhibited by the pore phase. Grain growth in spinel therefore follows the theoretical grain growth law rather than the usual cubic grain growth law.

If we assume that the average velocity of the spinel grain boundaries is proportional to dD/dt where D is the average grain diameter, then the relative grain boundary velocity can be determined as a function of stoichiometry. It was observed that the relative grain boundary velocity increased as the concentration of the Al_2O_3 increased in the spinel. A maximum in the grain boundary velocity occurred at approximately 83 wt% Al_2O_3 and the reasons for this maximum are discussed in the text.

The calculated grain boundary velocities are low and are consistent with Cahn's impurity drag theory for low-velocity grain growth with a

low driving force, in which the solute is assumed to be the excess oxide greater than the stoichiometric composition. Conformance to Cahn's theory suggests that the solute segregates to the grain boundaries as the solid solubility limit is approached. However, varying the stoichiometry of spinel within the limits of the $MgAl_2O_4$ phase field did not provide a spinel composition that exhibited sufficient grain growth inhibition to prevent discontinuous grain growth even though grain growth was inhibited as the composition approached the solid solubility limit.

$MgAl_2O_4$ can be sintered to theoretical density by the addition of a MgO second phase or other second phases that inhibit the grain boundary mobility. However, these second phases scatter light, and lower the in-line transmission, and as a result the spinel samples are opaque or translucent.

III EXPERIMENTAL PROCEDURE

Submicron oxide powders can be produced by calcining the appropriate carbonate, hydroxide, nitrate, oxalate, or sulfate salt at temperatures in the range of 1000° - 1300°C. The ultimate success in sintering an oxide to theoretical density depends critically on the starting materials since factors such as agglomeration, particle size, and particle size distribution affects the shrinkage kinetics and pore removal. For example Al_2O_3 powders obtained from calcination of carbonate, nitrate, hydroxide, or oxalate salts will not sinter to theoretical density as easily as alumina powders obtained from calcining of the sulfate salts. The ideal starting material would be a submicron-size powder with a uniform particle size so that the pore size would be small and uniformly distributed. Sintering experiments were therefore conducted with various starting materials to determine which spinel powder had the best sintering characteristics.

The evaluation procedure consisted of isostatically pressing the powders at 50,000 psi and sintering in a hydrogen atmosphere or an oxygen atmosphere for 16 hr at 1800°C. Samples were also sintered for 16 hr at 1900°C. Final densities were measured and metallographic sections were made to determine the final pore size and the final grain size.

Spinel powders were formed for evaluation using mixed oxide powders, and by calcining the following types of salts: carbonates, nitrates, sulfates, and hydrated ammonium aluminum sulfate mixed with hydrated magnesium nitrate. W. R. Grace & Co. spinel powder that was manufactured by a proprietary process was also evaluated. The evaluation data are shown in Table I.

All of the samples in Table I exhibited discontinuous grain growth,

Table I

SPINEL POWDERS

Starting Material	Calcining Temperature (°C)	Calcining Time (Hr)	Sintering Temperature	Sintering Time (CHr)	Final Density (g/cm^3)	Microstructural Features
$MgSO_4 \cdot 7H_2O$ + $Al_2(SO_4)_3 \cdot 9H_2O$	1100	1	1800	16	3.26	Pores in centers of grains
	1100	1	1900	16	3.36	
Al_2O_3 + $MgCO_3$ (Gatti Procedure)[13]	1250	1	1800	16	2.87	Large nonuniform pores
	1250	1	1900	16	3.10	
Grace Co. Spinel Powder (MgO/Al_2O_3 = 1.023)	-	-	1900	4	3.57	Small uniform pores in grains
Grace Co. Spinel Powder + $Mg(NO_3)_2 \cdot 6H_2O$	1000	1	1900	4	3.30	Small uniform pores in grains
$NH_4Al(SO_4)_2 \cdot 12H_2O$ + $Mg(NO_3)_2 \cdot 6H_2O$	1300	1	1900	4		Small uniform pores in grains

i.e., the grain boundaries break away from the pores and trap pores inside the grains of the sample. The oxide-derived powders had the lowest sintered density and the largest amount of nonuniform pores. The Grace Co. spinel powder sintered very well (see Table I); however, a second batch of material having a MgO/Al_2O_3 mole ratio of 1.056 did not sinter very well in that large pores formed inside the sample. This probably was due to incomplete calcination. Further work on Grace Co. spinel powders was discontinued because of the nonreproducibility.

Each of the above powders was also tested for its ability to form spinel powders having finely divided second phases of either magnesia or alumina. The ammonium aluminum sulfate plus magnesium nitrate mixed salts provided the best starting materials judging from the uniformity of the grains in the microstructure and the uniformity of the pores in the sintered samples. This material also yielded the most consistent particle size as a function of spinel composition and was therefore selected for the sintering study. The average particle size obtained as determined by a corrected Fisher analysis was 0.33 μm. Figure 5 is a scanning electron micrograph of the calcined spinel powder.

The composition of the spinel materials studied was varied from 60 wt% Al_2O_3 to 91 wt% Al_2O_3 by combining varying amounts of $NH_4Al(SO_4)_2 \cdot 12H_2O$ and $Mg(NO_3)_2 \cdot 6H_2O$. The ammonium aluminum sulfate and the magnesium nitrate melt at 93.5°C and 95°C, respectively. The aluminum and magnesium ions become intimately mixed in the liquid phase and on further heating to 1300°C the materials are decomposed to form finely divided spinel crystals approximately 0.3 μm in diameter. At calcining temperatures below 1300°C, the sintered samples expanded or bloated during sintering, which provided evidence that the calcining heat treatments below 1300°C were insufficient to decompose the sulfate salts.

FIGURE 5 SCANNING ELECTRON MICROGRAPH OF $MgAl_2O_4$ POWDER OBTAINED BY CALCINING A MIXTURE OF HYDRATED AMMONIUM ALUMINUM SULFATE AND HYDRATED MAGNESIUM NITRATE SALES (X20,000)

The calcined spinel powders were then isostatically pressed at 50,000 psi into cylindrical-shaped specimens and were packed in spinel powders of identical composition in covered molybdenum crucibles for firing in either a vacuum or hydrogen atmosphere. Spinel samples were also fired in an oxygen atmosphere at 1800°C using Al_2O_3 crucibles.

After firing, the samples were sectioned near the center of the sample, polished, and etched to reveal the microstructure. The grain size was determined by measuring the average length of random line intercepts across the grains, multiplied by a factor of 1.5.[20]

The densification of oxides is often enhanced by the addition of various solutes; therefore, several potential solutes were added to $MgAl_2O_4$ to investigate possible means of controlling the grain boundary mobility so that the material could be sintered to theoretical density. These solutes included Li_2O, LiF, Y_2O_3, and ZrO_2.

Spinel crystals often contain OH^- ions in the crystal lattice and therefore the hydroxyl concentration was followed in this study by monitoring the infrared absorption peaks at wavelengths of 2.5 to 3.5 μm.

IV RESULTS

Sintering of relatively pure oxide powders results in an entrapment of pores within the grains. A typical microstructure for $MgAl_2O_4$ is shown in Figure 6. This type of microstructure results from the grain boundaries breaking away from the pores, i.e., discontinuous grain growth. To sinter to theoretical density, discontinuous grain growth must be prevented, and the present program was initiated to investigate the possibility of preventing discontinuous grain growth by controlling the stoichiometry of the spinel phase. Evidence from other oxide systems such as Y_2O_3 and ThO_2 suggested that solute segregation to the grain boundaries increases as the chemical composition approaches the solid solubility limit. If we consider the solute in this system to be the MgO or Al_2O_3 in excess of the stoichiometric composition, we would expect the grain boundary mobility to decrease as the composition of the spinel phase approaches the solid solubility limits either on the MgO-rich side of the phase field or on the Al_2O_3-rich side of the phase field.

The grain boundary velocity, V, is related to the grain boundary mobility, μ, by the relationship

$$V = \mu P \qquad (2)$$

where P is the force causing the boundary to move. Grain boundaries move so that the total grain boundary area is decreased, i.e., the grain boundaries migrate toward their centers of curvature.

The grain boundaries are internal surfaces that can be described by two principal radii of curvature. The force, P, in Eq. (2) is therefore given by

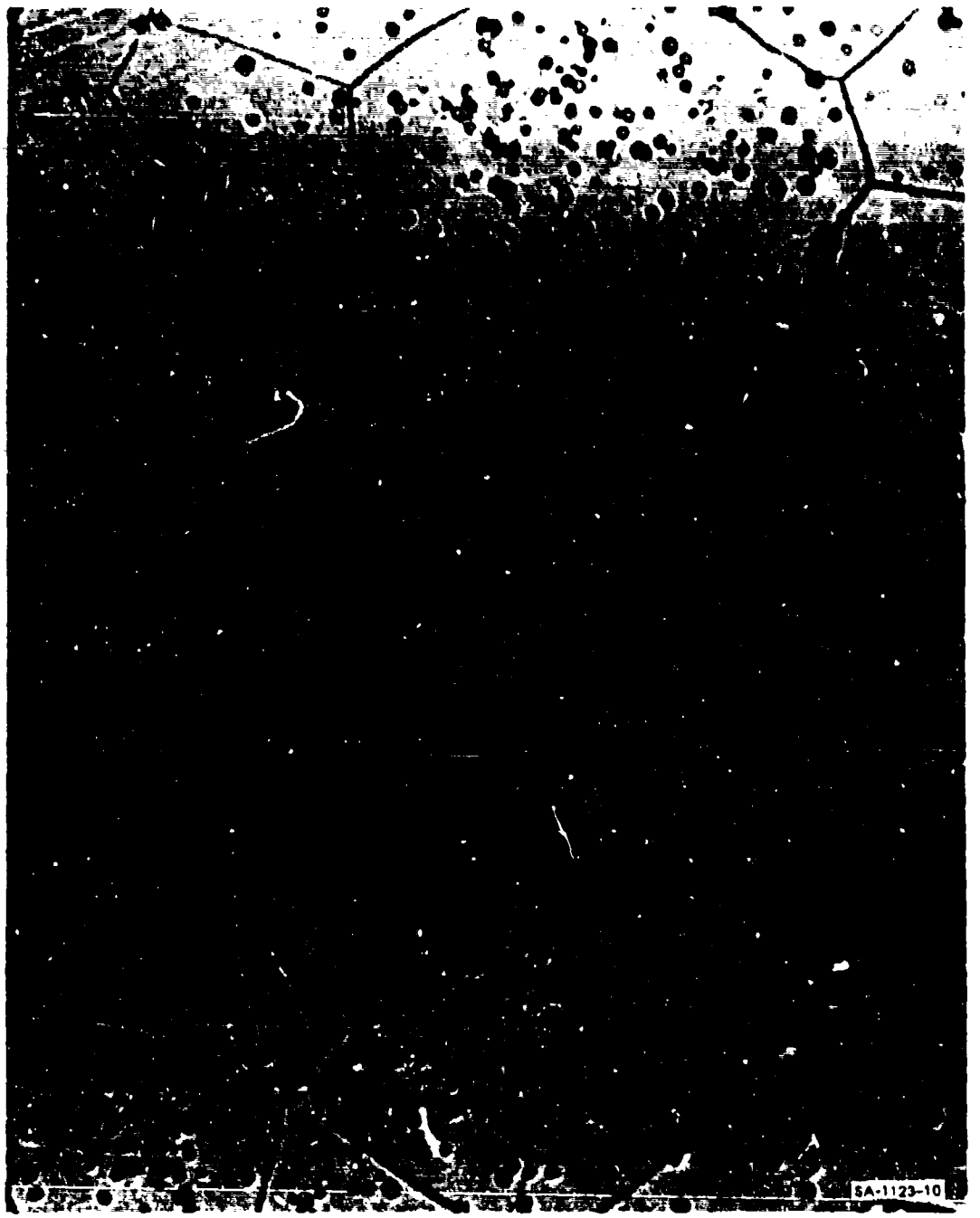

FIGURE 6 TYPICAL MICROSTRUCTURE OF SINTERED $MgAl_2O_4$ EXHIBITING DISCONTINUOUS GRAIN GROWTH (X1700)

$$P = 2\sigma(1/r_1 + 1/r_2) \qquad (3)$$

where σ is the grain boundary energy and r_1 and r_2 are the principal radii describing the grain boundary surface. Substituting Eq. (3) into Eq. (2) gives the following expression for the grain boundary velocity:

$$V = 2\mu\sigma(1/r_1 + 1/r_2) \quad . \qquad (4)$$

If we assume that V is proportional to dD/dt and that $(1/r_1 + 1/r_2)$ is proportional to 1/D where D is the average grain diameter, then

$$dD/dt = k'\mu\sigma/D \quad . \qquad (5)$$

Integration of Eq. (5) gives the theoretical grain growth equation,[21,22]

$$D^2 - D_o^2 = K\mu\sigma t \qquad (6)$$

where D_o is the initial average diameter at zero time.

The grain growth kinetics of $MgAl_2O_4$, follow the above derived grain growth law, as shown by Bratton's[15] data over the temperature range 1400° - 1600°C. The grain growth measurements made in this study are consistent with Bratton's data, and have been determined as functions of stoichiometry and time at 1900°C. Table II lists the grain growth values obtained as a function of stoichiometry at a constant time of 4 hours.

Grain growth kinetics in oxide systems often follow a cubic grain growth law, i.e.,

$$D^3 = At \qquad (7)$$

when coalescence or disappearance of the pore phase in the oxide controls the grain growth (see Hillert[23]). Since the grain growth kinetics in

Table II

GRAIN SIZE OF $MgAl_2O_4$ AS A FUNCTION OF STOICHIOMETRY*

Composition (wt% Al_2O_3)	Grain Size (μm)
63.0	12.7
65.0	17.5
68.0	13.5
71.8	20.8
79.1	28.1
85.5	31.3
91.0	18.1

the $MgAl_2O_4$ system do not follow Eq. (7) and because the rate of grain growth depends on the stoichiometry of the spinel, we can conclude that the grain growth kinetics are not influenced by the presence of porosity. Reasons why this is true will be presented in the discussion section.

The measurement of the grain growth kinetics as a function of time allow the relative velocity of the average grain boundary to be calculated if we assume that $dD/dt = V$, and this will provide a means of comparing relative grain boundary velocities at 1900°C as a function of stoichiometry. These data are shown in Figure ". The $MgAl_2O_4$ phase boundaries at 1900°C

*The grain sizes listed in Table II are the average grain diameters obtained for a temperature of 1900°C and a constant time of 4 hours.

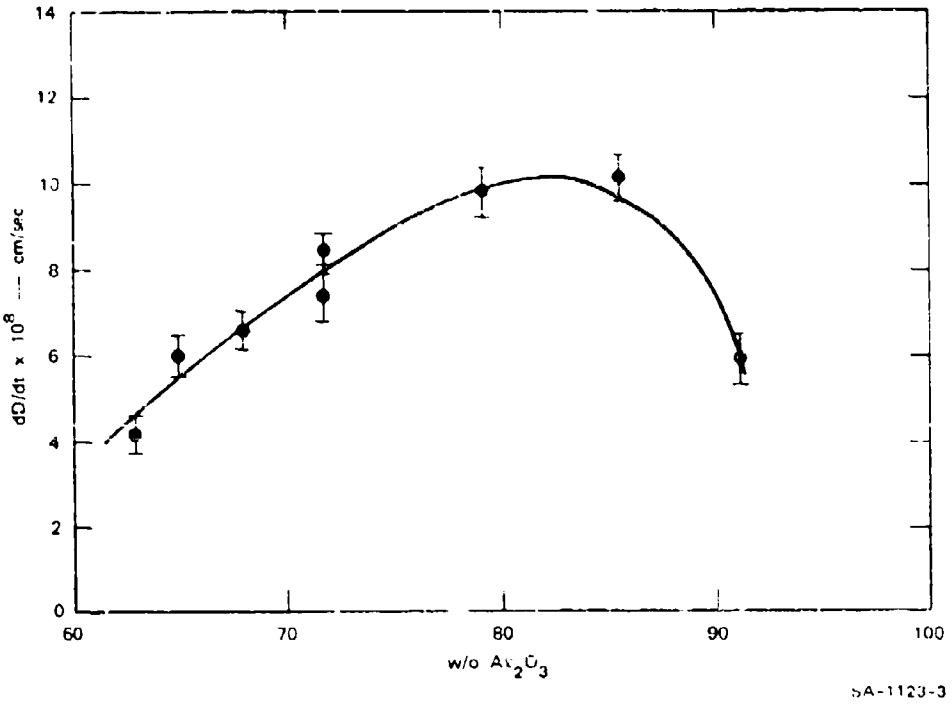

FIGURE 7 GRAIN BOUNDARY VELOCITY IN $MgAl_2O_4$ AT 1900°C AS A FUNCTION OF ALUMINA CONCENTRATION

occur at approximately 64 and 92 wt% Al_2O_3, thus all of the data points in Figure 7 except the 63 wt% Al_2O_3 point fall within the spinel phase field. The 63 wt% Al_2O_3 sample showed a second phase at three grain corners and in the centers of the grains, while the 65 wt% Al_2O_3 sample showed second phase in the center of the grains and only an occasional second-phase particle in the grain boundaries. Therefore, it is reasonable to conclude that the 65 wt% Al_2O_3 sample was single phase at 1900°C. The 91 wt% Al_2O_3 sample on cooling had large lath-like second phase grains that extended uninterrupted across the spinel grain boundaries. There were also small equiaxed second phase grains in the grain boundaries; however, the volume fraction of these latter grains was impossible to determine due to the extensive nature of the precipitated second phase grains. Thus it is impossible to conclude that the 91 wt% Al_2O_3 samples were single phase at 1900°C; i.e., we cannot assume that the 91 wt% Al_2O_3 samples were in equilibrium, and therefore the decrease in the grain boundary velocity as illustrated by the curve drawn in Figure 7 at high concentrations of Al_2O_3 may decrease too rapidly. However, it can be argued that the 85.5 wt% Al_2O_3 point shows a definite decrease, and that the grain-boundary velocity goes through a maximum as the spinel composition varies across the phase field.

Equation (1) provides a relationship between the grain boundary velocity and the solute concentration[12] for grain boundaries moving with low velocities. The reciprocal of Equation (1) is

$$1/V = \lambda/P + \alpha/PC_o \qquad (8)$$

and this expression predicts a linear relationship between the reciprocal of the grain boundary velocity and the solute concentration.

If the solute in the spinel system is considered to be the difference between the nonstoichiometric composition and the stoichiometric composition,

then the linearity of a plot of Eq. (8) will be maintained if the composition of the spinel phase is plotted versus the reciprocal velocity. Figure 8 is such a plot.

Since the datum point at 63 wt% Al_2O_3 is in a two-phase region (MgO + $MgAl_2O_4$), the linear relationship predicted by Eq. (8) should not pass through this particular point. The same argument can be given for the 91 wt% Al_2O_3 datum point. The remaining points form a good straight line when the error limits are considered indicating that Eq. (1) can describe the grain boundary velocity as a function of stoichiometry in spinel, and this suggests that solute segregation to the grain boundaries increases as the spinel composition approaches the solid solubility limit on the MgO-rich side of the spinel phase field.

Single crystal spinel grown by the Verneuil method contains hydroxyl groups[24] as evidenced by an infrared absorption peak at a wavelength of about 3 μm. Wang and Zanzvechi[25] observed that these absorption peaks occurred only in spinel crystals grown by the Verneuil technique and did not occur in flux or Czochralski-grown crystals. These authors therefore concluded that the 3-μm absorption band was not an intrinsic property of spinel. Jagodzinski[26] showed that there existed two absorption maxima in alumina-rich spinels corresponding to two energetically different O-H-O bonds. One of the absorption peaks occurs at 3.0 μm and the other peak occurs at 2.8 μm. The 2.8 μm peak as reported by Jagodzinski decreases with decreasing Al_2O_3 content and disappears at the stoichiometric composition. Since a changing hydroxyl concentration can alter the defect structure and thereby influence the solute segregation to grain boundaries and hence affect the sintering kinetics, the hydroxyl concentration was monitored in the polycrystalline-sintered samples. Only one absorption peak was observed at a wavelength of 2.9 μm (see Figure 9) regardless of the spinel composition. The infrared absorption of MgO-rich spinel was measured between 60 and 70 wt% Al_2O_3 for samples fired at 1800°C. These

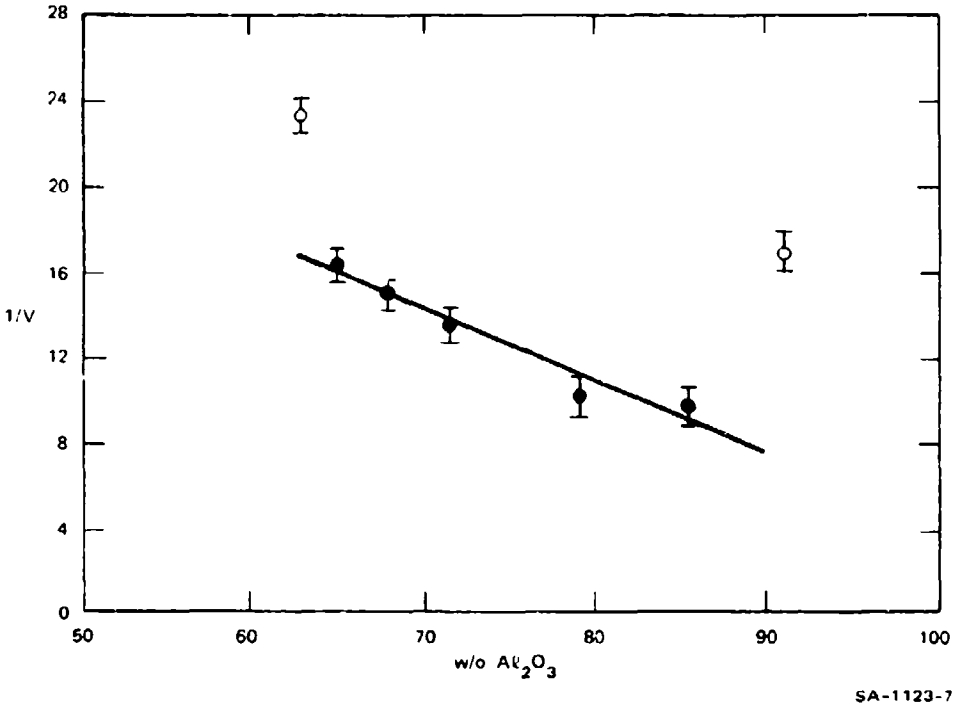

FIGURE 8 A PLOT OF THE RECIPROCAL OF THE GRAIN BOUNDARY VELOCITY AS A FUNCTION OF ALUMINA CONCENTRATION

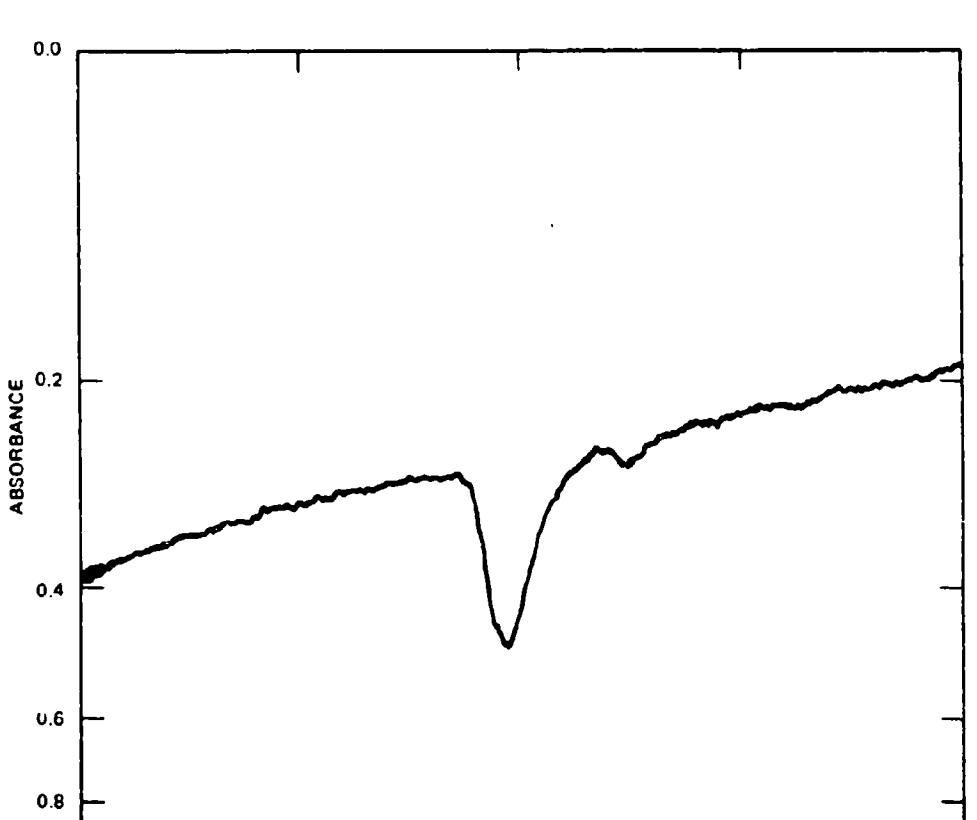

FIGURE 9 INFRARED ABSORPTION SPECTRA OF $MgAl_2O_3$

data are shown in Figure 10 as a function of wt% MgO. The break in the curve in Figure 10 corresponds exactly to the solid solubility limit at 1800°C. The significance of the hydroxyl concentration decreasing as the MgO concentration in the spinel phase increases will be presented in the discussion section.

Since Wang and Zanzvechi[25] did not observe hydroxyl groups in stoichiometric crystals grown by the flux or by the Czochralski methods, we investigated the effect of the sintering atmosphere on the hydroxyl concentration. The absorption band at 2.9 μm was present in the spinel samples sintered at 1800°C regardless of the sintering atmosphere. Samples were sintered in hydrogen, oxygen, and in a vacuum of 10^{-5} torr at 1800°C. The OH^- peak heights were identical for either a hydrogen or an oxygen sintering heat treatment, and therefore the hydroxyl ions incorporated into the spinel crystals during the calcining procedure are not easily removed. The data shown in Figure 10 were obtained on samples sintered in 750 torr of oxygen at 1800°C.

Sintering spinel samples with large deviations from stoichiometry did not provide sufficient reduction in the grain boundary mobility to achieve theoretical density and on cooling the MgO-rich spinel samples contained a precipitated MgO second phase. The minor amount of residual porosity and small second-phase precipitates shown in the micrograph of Figure 11 cause light scattering to such an extent that the samples exhibit less than 5% in-line transmission for a sample 1 mm thick. Dopants were therefore added to spinel in an attempt to find an additive that would go into solid solution and simultaneously inhibit grain growth, since these two requirements are necessary to achieve a transparent, theoretically dense, oxide material.

The additives selected for investigation were Li_2O, LiF, Y_2O_3 and ZrO_2. The lithium compounds were added in an attempt to increase the concentration of anion vacancies and the zirconia was added to inc[illegible]se

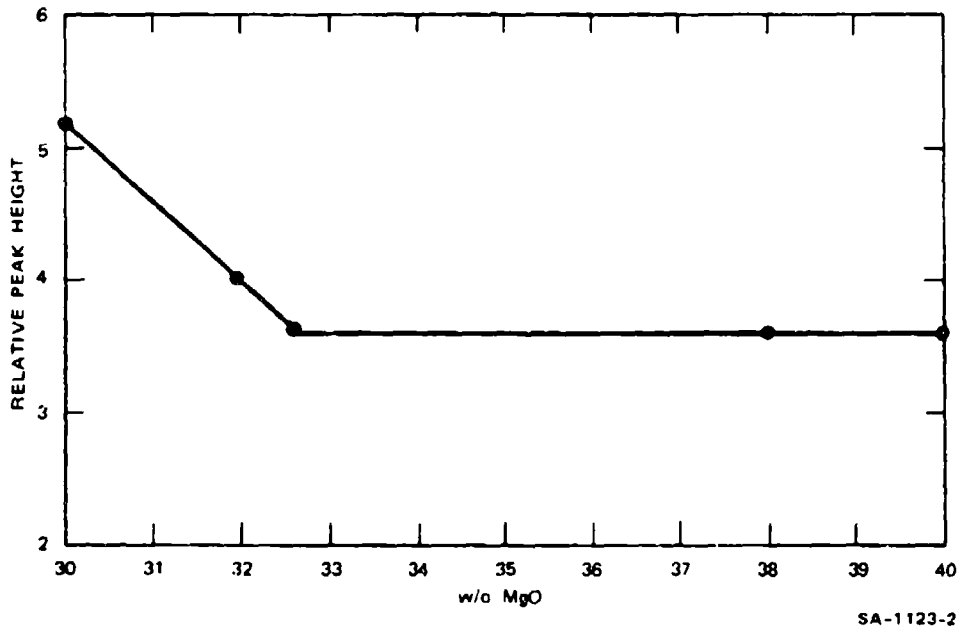

FIGURE 10 A PLOT OF THE RELATIVE PEAK HEIGHT AT A WAVELENGTH OF 2.9 μm IN $MgA\ell_2O_4$ AS A FUNCTION OF MgO CONCENTRATION

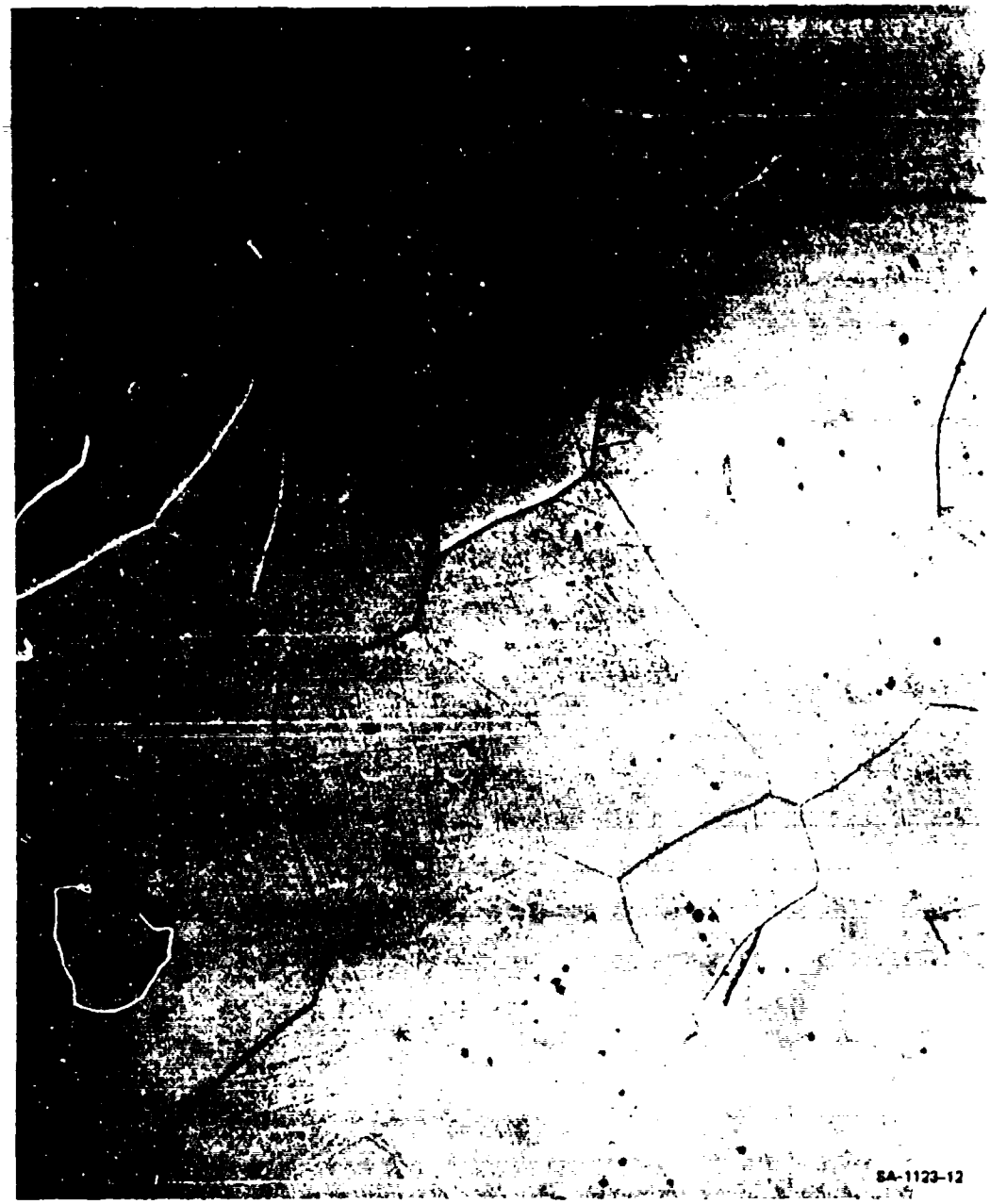

FIGURE 11 TYPICAL MICROSTRUCTURE OF A NONSTOICHIOMETRIC SINTERED $MgAl_2O_4$ IN THE MgO-RICH SPINEL PHASE FIELD (X850)

the cation vacancy concentration. Y_2O_3 was added to MgO-rich spinel samples to investigate whether a liquid-phase addition would increase the sintering kinetics sufficiently to prevent discontinuous grain growth. The yttria additions produced a liquid phase as evidenced by the structure at the triple point in the micrograph shown in Figure 12. The pores in the centers of the grains of Figure 12 provide evidence that discontinuous grain growth occurred in this sample.

The Li_2O, LiF, and ZrO_2 were each added to separate spinel samples of stoichiometric composition and also to 68 wt% Al_2O_3 spinel. The concentration of the additives was varied between 1 and 3 wt%. In all cases pore coalescence occurred as seen in Figure 13 and the samples did not sinter to theoretical density after firing at 1900°C for 16 hours. If a second phase was present, then sintering to theoretical density could be achieved; however, the second-phase particles scattered light and the resulting samples were translucent.

Sintering of spinel containing a MgO second phase allowed sintering to proceed to theoretical density through the operation of the second phase pinning the grain boundaries and allowing a relatively high diffusion flux to remove all of the porosity. These samples were opaque to translucent due to the scattering of light by the extensive second phase. This phenomenon was not investigated further, because one of the objectives of this research was to produce transparent spinel.

FIGURE 12 MICROSTRUCTURE OF Y_2O_3 DOPED $MgAl_2O_4$ (X850)

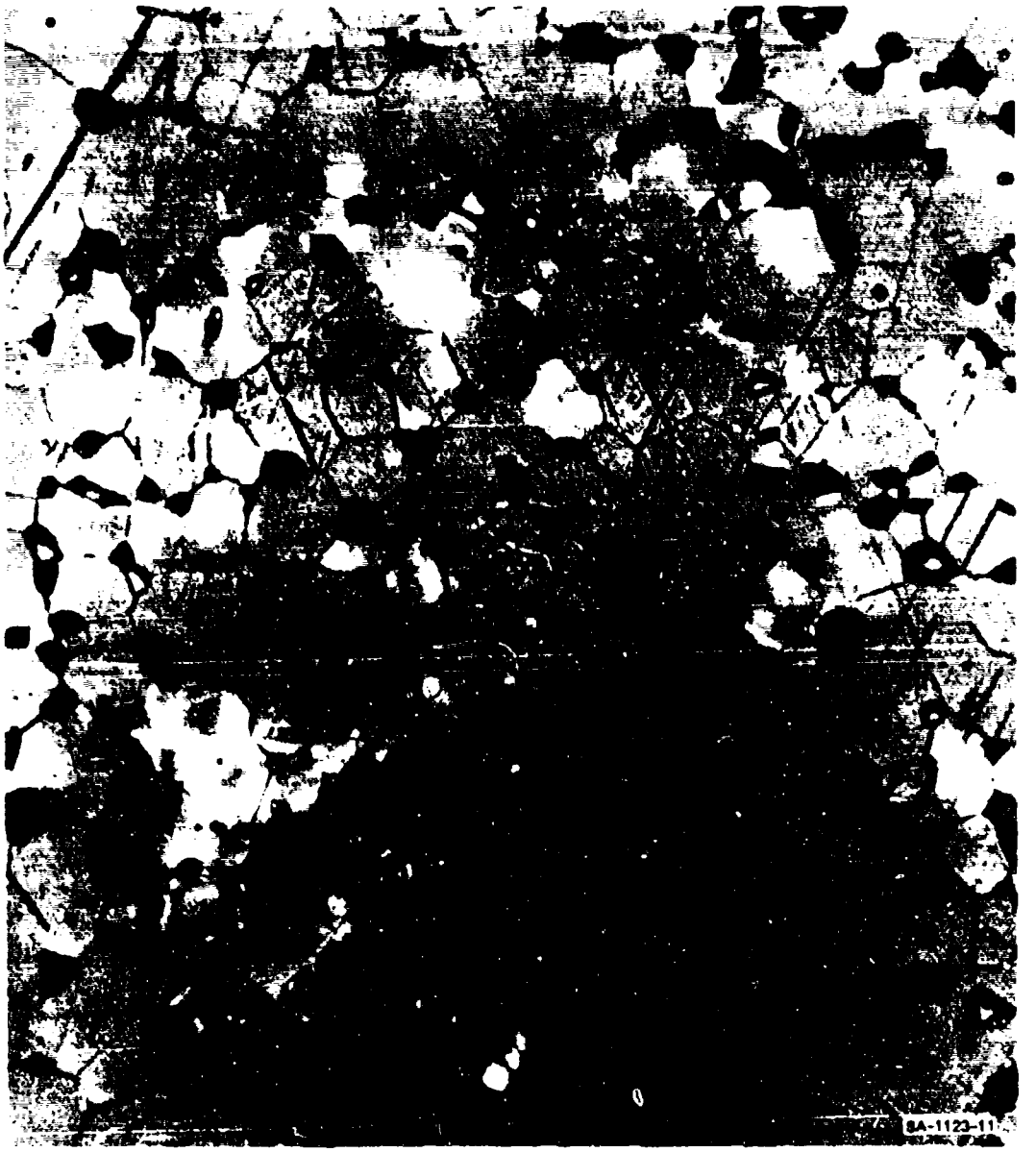

FIGURE 13 TYPICAL MICROSTRUCTURE OF $MgAl_2O_4$ EXHIBITING PORE COALESCENCE (X850)

V DISCUSSION

The principal defects in Al_2O_3-rich spinel according to Jagodzinski and Saalfeld[27] are aluminum cation vacancies and the defect equilibria can be described by the following equation,

$$3Mg^{++} \rightleftharpoons 3Al^{+++} + V_{Al}^{'''} \tag{9}$$

where $V_{Al}^{'''}$ represents a fully ionized aluminum ion vacancy.

It is reasonable to assume that anion vacancies occur in MgO-rich spinel according to the equation,

$$2Al^{+++} \rightleftharpoons 2Mg^{++} + V_O^{\cdot\cdot} \tag{10}$$

where $V_O^{\cdot\cdot}$ is a doubly ionized oxygen vacancy. However, it is also possible that three magnesium ions substitute for two aluminum ions with the extra magnesium ion occupying a normally empty tetrahedral site.

The excess magnesium ions in MgO-rich spinel or the excess aluminum ions in Al_2O_3-rich spinel will be distributed in the spinel lattice and on the existing grain boundaries. As the composition approaches the solid solubility limit, the concentration of the excess cations in the grain boundaries could increase more rapidly than the excess concentration in the lattice and this increased concentration at grain boundaries is postulated to exert a drag on the grain boundary mobility. This model would thus predict a maximum in the grain boundary velocity at the stoichiometric composition, and this was not observed.

The grain boundary velocity data were calculated from the rate of grain growth in a hydrogen atmosphere, and therefore it is possible that a significant concentration of anion vacancies exists at the stoichiometric

composition. If we postulate that the anion vacancy concentration at the stoichiometric composition is not nil, then Eq. (10) could describe the defect equilibria beyond the MgO-rich spinel region into the Al_2O_3-rich spinel region. The maximum in grain boundary velocity observed in Fig. 7, could be explained on this basis.

If the 91 wt% Al_2O_3 grain growth samples were actually in equilibrium, then two straight lines should have been drawn through the data in Fig. 8, with a minimum occurring in the reciprocal grain boundary velocity at approximately 83 wt% Al_2O_3. However, the existence of second-phase grains in the spinel grain boundaries of these samples having a different morphology than the precipitated grains strongly suggests that equilibrium did not occur and that Fig. 8 is correct as drawn.

The straight-line relationship exhibited in Fig. 8 suggests a solute segregation involving anion vacancies, and provides evidence that the grain boundary velocity decreases as the composition approaches the solid solubility limit. However, this reduction in grain boundary velocity was insufficient to allow the spinel to sinter to theoretical density or it was insufficient to prevent discontinuous grain growth. This could be due to the fact that the densification kinetics in $MgAl_2O_4$ are slow (compare the slowest diffusion coefficients in Figs. 1 and 4), or it could be due to the replacement of cations by protons in the spinel lattice making the spinel system a four-component system with insufficiently controlled activity of the components which could affect the segregation of solute-defect clusters to grain boundaries.

The data in Fig. 10 clearly demonstrate that the hydroxyl concentration decreases as the amount of excess MgO in MgO-rich spinel increases. Jagodzinski[26] has observed a similar phenomenon in Al_2O_3-rich spinels, and an equation that could describe this phenomenon is

$$H_2 + 2O^{=} \rightleftharpoons Mg\uparrow + 2(OH^{-}) + V''_{Mg} \qquad (11)$$

in which two protons substitute for a magnesium ion in the spinel lattice.

A cubic grain growth law was not observed in porous spinel and because this is unusual it merits discussion. Burke[22] has written an excellent treatise on this topic, in which he gives the following grain growth law, for porous compacts

$$dD/dt = k\mu\sigma(1/D - 1/D_\ell) \tag{12}$$

where D_ℓ is the average limiting grain size determined by a Zener-type relationship,

$$D_\ell = d/f \tag{13}$$

in which d is the average diameter of the pores and f is the volume fraction of pores.

The diameter of the pores and their volume fraction change during sintering; for example, the volume fraction decreases as densification occurs and we know that the pores in $MgAl_2O_4$ coalesce (see Fig. 13). Both of these phenomena cause the average limiting grain size, D_ℓ, to increase. It is therefore hypothesized that the term $1/D_\ell$ in Eq. (12) is negligible with respect to the 1/D term for the spinel system, and therefore Eq. (12) becomes equal to Eq. (5) and we observe the grain growth behavior predicted by Eq. (6).

Bagley[14] sintered spinel to theoretical density by adding small amounts of excess MgO to the stoichiometric composition. The mechanism by which theoretical density was achieved had to be one in which a nonequilibrium second phase inhibited the grain boundary mobility, and this sintering procedure did not produce a transparent spinel. Gatti[13] and Bratton[28] have both produced theoretically dense spinel using additives that result in a liquid phase, but unless the liquid phase can be

removed, and this was Gatti's approach, the spinel will not be transparent. For example, Bratton used CaO additives and in his best material obtained approximately 30% - 35% in-line transmission for a 1-mm-thick sample, which is inadequate for window or armor applications.

REFERENCES

1. B. H. Alexander and R. W. Balluffi, "Mechanism of Sintering of Copper," Acta Met. 5 666 (1957)

2. J. E. Burke, "Role of Grain Boundaries in Sintering," J. Amer. Ceram. Soc. 40 (3) 80-85 (1957)

3. L. Seigle, Kinetics of High-Temperatures Processes, pp. 172-178, edited by W. D. Kingery. (Technology Press of Massachusetts Institute of Technology, Cambridge, and John Wiley & Sons, Inc., New York, 1959)

4. H. G. Van Bueren and J. Hornstra, Reactivity of Solids, p. 112, edited by J. H. deBoer, W. G. Burgers, E. W. Gorter, J.P.F. Huesse, and G.C.A. Schmit (Elsevier Publishing Co., Princeton, J.H., 1961)

5. R. L. Coble and J. E. Burke, pp. 197-251 in Progress in Ceramic Science, Vol. 3, edited by J. E. Burke. (Pergamon Press, New York 1964)

6. R. L. Coble, "Sintering Crystalline Solids: I" J. Appl. Phys. 32 (5) 787-92 (1961); II ibid., pp. 793-99

7. P. J. Jorgensen and R. C. Anderson, "Grain-Boundary Segregation and Final-Stage Sintering of Y_2O_3," J. Amer. Ceram. Soc. 50 (11) 553-58 (1967)

8. P. J. Jorgensen and W. C. Schmidt, J. Amer. Ceram. Soc. 53 24 (1970)

9. R. C. Anderson, U.S. Patent 3,574,645, April 13, 1971

10. P.J.L. Reijnen, Problems of Nonstoichiometry, edited by A. Rabeneau, p. 219 (North Holland Publishing Co., Amsterdam, 1970)

11. P. J. Jorgensen and J. H. Westbrook, J. Amer. Ceram. Soc. 47 332 (1964)

12. J. W. Cahn, Acta Met. 10 784 (1962)

13. A. Gatti, R. L. Mehan and M. J. Noone, "Development of a Process for Producing Transparent Spinel Bodies," Naval Air Systems Command Report, Contract No. N00019-71-C-0126 (Dec. 1971)

14. R. D. Bagley, U.S. Patent 3,531,308, Sept. 29, 1970

15. R. J. Bratton, J. Amer. Ceram. Soc. 54 141 (1971)

16. R. J. Bratton, J. Amer. Ceram. Soc. 52 417 (1969)

17. Lindner unpublished preliminary results, see Z. Physik. Chem. Neue Folge 18 303 (1958)

18. Y. Oishi, personal communication

19. K. Ando and Y. Oishi, Yogyo-Kyokai-Shi 80 324 (1972)

20. R. L. Fullman, Trans. AIME 197 447 (1953)

21. J. E. Burke and D. Turnbull, Progress in Metals Physics, Vol. III, edited by Bruce Chalmers, p. 220 (Pergamon Press, London, 1952)

22. J. E. Burke, "Ceramic Microstructures," Proc. 3rd Int. Mater. Symp., Berkeley, Calif., p. 681, June 1966

23. M. Hillert, Acta Met. 13 227 (1965)

24. K. A. Wickersheim and R. A. Lefever, J. Opt. Soc. Am. 50 831 (1960)

25. C. C. Wang and P. J. Zanzucchi, J. Electrochem. Soc. 118 586 (1971)

26. H. Jagodzinski, Problems of Nonstoichiometry, edited by A. Rabeneau, p. 131 (North-Holland Publishing Co., Amsterdam, 1970)

27. H. Jagodzinski and H. Saalfeld, Z. Krist. 110 197 (1958)

28. R. J. Bratton, "Transparent Sintered $MgAl_2O_4$ "to be published)

29. D. M. Roy, R. Roy, and E. F. Osburn, J. Amer. Ceram. Soc. 36 149 (1953)

30. A. M. Alper, R. N. McNally, P. G. Ribbe, and R. C. Doman, J. Amer. Ceram. Soc. 45 264 (1962).